A New Tripodal Tetradentate Ligand and Its Iron(III) Complex, as a Model for Mononuclear Non-Heme Iron Active Sites. Reactivity Studies toward Dioxygen and Superoxide

Marie-Carmen Rodriguez and Irène Morgenstern-Badarau*

Laboratoire de Chimie Bioorganique et Bioinorganique, Institut de Chimie Moléculaire d'Orsay, Université Paris-Sud, 91405 Orsay, France

Michèle Cesario and Jean Guilhem

Institut de Chimie des Substances Naturelles, CNRS, 91198 Gif-s/-Yvette, France

Bineta Keita and Louis Nadjo

Laboratoire d'Electrochimie et de Photoélectrochimie, Institut de Chimie Moléculaire d'Orsay, Université Paris-Sud, 91405 Orsay, France

Received August 11, 1995[⊗]

The new biomimetic ligand (bis((1-methylimidazol-2-yl)methyl)amino)acetic acid (LH) has been synthesized, which increases the growing family of tripodal tetradentate ligands. Reaction of LH with $FeCl_3 \cdot 6H_2O$ allowed us to obtain the corresponding iron(III) complex $[Fe(L)Cl_2]$. The crystal structure reveals mononuclear neutral molecules with four chiral molecules per asymmetric unit (crystal data: monoclinic, $P2_1$, $a = 12.564(5)$ Å, $b = 25.960(10)$ Å, $c = 9.875(4)$ Å, $\alpha = 90.00°$, $\beta = 60.494(4)°$, $\gamma = 90.00°$, $V = 3221(2)$ Å^3, $Z = 8$, $R = 0.0601$ for 2433 unique reflections with $F_o > 4\sigma(F)$ and 452 variable parameters). The iron(III) center is located in a distorted octahedral environment consisting of four donor atoms from the ligand **L**, two imidazole nitrogens, an amine nitrogen, and one oxygen of the carboxylate group, with the 6-fold coordination being completed by two chloride anions. UV−vis and EPR spectra are solvent dependent due to the two labile chloride positions. Cyclic voltammograms run under an argon atmosphere exhibit a one-electron quasi-reversible redox process ($E° = -0.015$ V *vs* SCE in DMSO). The reaction of the complex with dioxygen and superoxide has been investigated through UV−vis spectroscopic and electrochemical studies. Direct UV−vis spectroscopic observations upon reaction with potassium superoxide, KO_2, dissolved in DMSO indicate that a new species is formed, symbolyzed $[Fe(III)-O_2^-]$. Comparison of the cyclic voltammograms obtained under argon or in the presence of dioxygen unambiguously indicates that the reduced form of the complex reacts with dioxygen. The buildup of a new species is confirmed by controlled potential electrolysis experiments of the associated voltammograms in the presence of dioxygen. This new species, symbolyzed $[Fe(II)-O_2]$, has been shown to be stable even in the absence of dioxygen. Its UV−vis spectrum is superimposable with the spectrum of $[Fe(III)-O_2^-]$, indicating that the same oxygenated entity has been formed. Reaction of superoxide with the iron(III) complex has also been monitored through cyclic voltammetry, which confirms that superoxide is reactive toward the complex.

Introduction

Mononuclear non-heme iron proteins possess common underlying features, especially with regard to the coordination of the iron center.[1] In most of them, the chelating atoms are nitrogen from histidine residues and oxygen from carboxylate or phenolate residues. The variation in the composition of the ligand sets can modulate the reactivity of the corresponding enzymes. On the other hand, according to the structural information now available, there are iron active sites that contain structural similarities but have various functions. Striking examples are the enzymes iron superoxide dismutases[2] and lipoxygenases.[3,4] In both kinds of proteins, the iron center is surrounded by a N_3O_1 set of ligand donors from three histidines and one carboxylate group. In the case of FeSOD from *Pseudomonas ovalis*, the active site structure is best described as distorted tetrahedral, the carboxylate group being an aspartate.[2d,e] A water molecule or a hydroxy ligand is found at the fifth position in FeSOD from *Escherchia coli*, and then the geometry is close to trigonal bipyramidal.[2a−c,f] Two crystal structures of soybean lipoxygenase have been reported. In both structures, the N_3O_1 amino acid ligands, namely three histidines and one isoleucine (through the C-terminal carboxylate), are

* Author to whom correspondence should be addressed.

⊗ Abstract published in *Advance ACS Abstracts,* December 1, 1996.

(1) (a) Feig, A. L.; Lippard, S. J. *Chem. Rev.* **1994**, *94*, 756. (b) Que, L., Jr. *Struct. Bonding (Berlin)* **1980**, *40*, 39.

(2) (a) Tierney, D. L.; Fee, J. A.; Ludwig, M. L.; Penner-Hahn, J. E. *Biochemistry* **1995**, *34*, 1661. (b) Lah, M. S.; Dixon, M. M.; Pattridge, K. A.; Stallings, W. C.; Fee, J. A.; Ludwig, M. L. *Biochemistry* **1995**, *34*, 1646−1660. (c) Stallings, W. C.; Metzger, A. L.; Pattridge, K. A.; Fee, J. A.; Ludwig, M. L. *Free Radical Res. Commun.* **1991**, *12*−*13*, 259−268. (d) Stoddard, B. L.; Howell, P. L.; Ringe, D.; Petsko, G. A. *Biochemistry* **1990**, *29*, 8885−8893. (e) Ringe, D.; Petsko, G. A.; Yamakura, F.; Suzuki, K.; Ohmori, D. *Proc. Natl. Acad. Sci. U.S.A.* **1983**, *80*, 3879−3883. (f) Stallings, W. C.; Powers, T. B.; Pattridge, K. A.; Fee, J. A.; Ludwig, M. L. *Proc. Natl. Acad. Sci. U.S.A.* **1983**, *80*, 3884−3888.

(3) Boyington, J. C.; Gaffney, B. J.; Amzel, L. M. *Science* **1993**, *260*, 1482−1486.

(4) Minor, W.; Steczko, J.; Bolin, J. T.; Otwinowski, Z.; Axelrod, B. *Biochemistry* **1993**, *32*, 6320−6323.

S0020-1669(95)01060-3 CCC: $12.00

conserved. In one of the published structures, the iron active site has been described as four coordinate,[3] while a fifth ligand, an asparagine residue with a relatively long bond length, has been identified in the other one.[4]

In order to mimic this protein environment, we have focused on nitrogen-centered tripodal tetradentate ligands. A variety of these kinds of ligands have been used to synthesize either mononuclear[5] or binuclear[6] iron model compounds, which have brought considerable insight into the properties of non-heme iron proteins. Some of these tripodal tetradentate ligands include imidazole functions as pendant groups.[6b,7] However, to date, none of them has combined both imidazole groups and an acid function. We have synthesized a new biomimetic ligand containing the two functionalities and its iron(III) complex. We report here the route to the synthesis of the tripodal tetradentate ligand (bis((1-methylimidazolyl)methyl)amino)acetic acid (LH), and the complex $[Fe^{III}(L)Cl_2]$, abbreviated FeL. This complex has been characterized by X-ray analysis, spectroscopic, and electrochemical studies. It represents a reasonable structural model for the above cited non-heme active sites.[2,3] Its reactivity toward dioxygen and superoxide has been investigated.

Experimental Section

Materials and Procedures. Ethyl bromoacetate (97%), 1-methylimidazole (99%), *n*-butyllithium (1.6 M solution in hexane), and $FeCl_3 \cdot 6H_2O$ were purchased from Jansen Chimica and used as received. All solvents were reagent grade and used without further purification except when indicated, in which case the solvents were dried by standard procedures.

Synthesis of the Ligand (Bis((1-methylimidazol-2-yl)methyl)-amino)acetic Acid (LH). This compound was obtained by alkylation of bis(2-(1-methylimidazolyl)methyl)amine (**1**) to form ((ethoxycarbonyl)methyl)bis(2-(1-methylimidazolyl)methyl)amine (**2**) followed by the hydrolysis of **2**.

Bis(2-(1-methylimidazol-2-yl)methyl)amine (1). A solution of 1-methyl-2-imidazolcarboxaldehyde oxime (6.25 g, 0.05 mol), prepared according to the published procedure,[8] in nonanhydrous methanol (150 mL) was hydrogenated at atmospheric pressure and room temperature over 10% palladium charcoal for 5 days. The catalyst was filtered and washed with methanol (20 mL), and the filtrate was evaporated to give a white powder, which is digested in 80 mL of hexane to remove impurities. Yield: 80%. Mp: 120 °C. MS: strong peak at $m/z = 206$ ($M + 1$). ^{1}H NMR (in $CDCl_3$), δ (ppm): 2.23 (s, 1H, NH); 3.60 (s, 6H, $-CH_3$); 3.84 (s, 4H, $-CH_2$); 6.79 (d, 2H, H_{Im}); 6.90 (d, 2H, H_{Im}). ^{13}C NMR (in $CDCl_3$), δ (ppm): 32.56 (s, 2C, N$-CH_3$); 44.56 (s, 2C, N$-CH_2-$Im); 121.2 (s, 2C, C_{4-Im}); 127.05 (s, 2C, C_{5-Im}); 146.10 (s, 2C, C_{2Im}).

((Ethoxycarbonyl)methyl)bis(2-(1-methylimidazolyl)methyl)-amine (2). Potassium carbonate (2.76 g, 0.02 mol) and ethyl bromoacetate (1.22 mL, 0.011 mol) were added to a solution of **1** (2.05 g, 0.01 mol) in anhydrous dimethylformamide (30 mL) under an argon atmosphere. The resulting suspension was sheltered from light and stirred for 12 h at 30 °C followed by 24 h at room temperature. After the suspension was filtered, the solvent was evaporated and the resulting red oil was purified by gel chromatography. A mixture of dichloromethane and methanol in a 95:5 to 85:15 ratio was used as the eluant to give 1.3 g of a white powder. Yield: 42%. ^{1}H NMR (in $CDCl_3$), δ (ppm): 1.20 (t, 3H, CH_2-CH_3); 3.37 (s, 2H, CH_2COOEt); 3.53 (s, 6H, N$-CH_3$); 3.77 (s, 4H, CH_2-Im); 4.06 (q, 2H, CH_2-CH_3); 6.80 (d, 2H, H_{Im}); 6.88 (d, 2H, H_{Im}). ^{13}C NMR (in $CDCl_3$), δ (ppm): 14.12 (s, 1C, CH_2CH_3); 32.48 (s, 2C, N$-CH_3$); 49.95 (s, 2C, N$-CH_2-$Im); 54.63 (s, 1C, N$-CH_2-$COO); 60.46 (s, 1C, CH_2CH_3); 121.67 (s, 2C, C_{4Im}); 127.28 (s, 2C, C_{5Im}); 144.67 (s, 2C, C_{2Im}); 171.00 (s, 1C, $-$COO).

(Bis((1-methylimidazol-2-yl)methyl)amino)acetic Acid (LH). A solution of **2** (0.56 g, 0.0019 mol) in methanol (10 mL) was added to a solution of potassium carbonate (0.58 g, 0.004 mol) in water (35 mL). The resulting solution was stirred for 5 days at room temperature. Then the solvent was evaporated to half its volume and washed with 2×10 mL of dichloromethane. A 0.1 M aqueous solution of HCL (80 mL, 8 mmol) was added. The pH of the degassed solution was 6.5. This indicates that the ligand is probably present as a zwitterion. The solution was lyophilized, and the resulting powder was extracted by anhydrous methanol. We checked that the amount of the remaining white solid, identified as KCl, corresponded to the amount of HCl introduced. This confirms the formation of an intramolecular zwitterion without additional counterions. Evaporation of the solvent gives 0.45 g of a white hygroscopic powder. Yield: 90%. ^{1}H NMR (in D_2O), δ (ppm): 2.87 (s, 2H, CH_2COOH); 3.30 (s, 6H, N$-CH_3$); 3.50 (s, 4H, CH_2-Im); 6.65 (d, 2H, H_{Im}); 6.78 (d, 2H, H_{Im}). ^{13}C NMR (in D_2O), δ (ppm): 33.07 (s, 2C, N$-CH_3$); 49.68 (s, 2C, N$-CH_2-$Im); 58.58 (s, 1C, N$-CH_2-$COO); 65.03 (s, 1C, CH_2CH_3); 123.42 (s, 2C, C_{4Im}); 126.82 (s, 2C, C_{5Im}); 145.87 (s, 2C, C_{2Im}); 179.10 (s, 1C, $-$COO).

Synthesis of the Complex $[Fe^{III}(L)Cl_2]$. The complex was obtained by dissolving LH (0.131 g, 0.5 mmol), $FeCl_3 \cdot 6H_2O$ (0.135 g, 0.5 mmol), and piperidine (20 μL, 0.2 mmol) in anhydrous methanol (20 mL) under an argon atmosphere. The solution was heated to reflux for 30 min to give a yellow precipitate, which was filtered off and washed with anhydrous methanol (10 mL). Yield: 60%. Anal. Calcd for $C_{12}H_{16}N_5O_2FeCl_2$: C, 37.05; H, 4.15; N, 18.0; Fe, 14.35; Cl, 18.22. Found: C, 37.06; H, 4.18; N, 17.90; Fe, 13.39; Cl, 18.04. IR (cm^{-1}): ν_{as}(C=O), 1656; ν_s(O$-$C$-$O), 1339; ν(C=N), 1500, 1516.

In order to obtain crystals suitable for X-ray analysis, synthesis was performed in an acetonitrile$-$methanol solution without addition of piperidine. The solution was heated to reflux for 1 h. The temperature was then allowed to decrease slowly within 24 h to give yellow monocrystals.

Crystallographic Studies. X-ray diffraction data were collected at room temperature on a yellow crystal of FeL with dimensions $0.20 \times 0.20 \times 0.20$ mm^3. The crystal was mounted on a Phillips PW 1100 diffractometer equipped with a graphite-monochromated Mo Kα radiation ($\lambda = 0.710\,70$ Å). Accurate cell parameters, obtained from least-squares refinement, are reported in Table 1 with the other pertinent details for the structure determination. The structure was solved by direct methods (program SHELXS86)[9] and refined on F^2 for all reflections by a least-squares method, using SHELXL-93.[10] Hydrogen atoms, located on difference synthesis, were refined as riding model with an isotropic thermal factor equivalent to 1.1 of the bonded atom. Only Fe, Cl, and O atoms were refined anisotropically to limit the number of parameters versus the number of data. The final conventional R factor was $R = 0.0601$ for 2433 unique reflections with $F_o > 4\sigma(F)$ and 452 variable parameters.

Selected bond distances and angles are collected in Table 2. A complete listing of the atomic coordinates and equivalent isotropic displacement parameters, bond lengths and bond angles, and anisotropic thermal parameters are supplied as Supporting Information.

Physical Methods. Electronic absorption spectra were recorded on a Safas double-mode spectrophotometer in DMSO, DMF, or acetoni-

(5) See, for example: (a) Cox, D. D.; Que, L., Jr. *J. Am. Chem. Soc.* **1988**, *110*, 8085−8092. (b) Jang, H. G.; Cox, D. D.; Que, L., Jr. *J. Am. Chem. Soc.* **1991**, *113*, 9200−9204. (c) Randall, C. R.; Zang, Y.; True, A. E.; Que, L., Jr.; Charnock, J. M.; Gardner, C. D.; Fujishima, Y.; Schofield, C. J.; Baldwin, J. E. *Biochemistry* **1993**, *32*, 6664−6673. (d) Leising, R. A.; Norman, R. E.; Que, L., Jr. *Inorg. Chem.* **1990**, *29*, 2553−2555. (e) Chiou, Y.-M.; Que, L., Jr. *J. Am. Chem. Soc.* **1995**, *117*, 3999−4013.

(6) See, for example: (a) Wilkinson, E. C.; Dong, Y.; Que, L., Jr. *J. Am. Chem. Soc.* **1994**, *116*, 8394. (b) Buchanan, R. M.; Chen, S.; Richardson, J. F.; Bressan, M.; Forti, L.; Morvillo, A.; Fish, R. H. *Inorg. Chem.* **1994**, *33*, 3208. (c) Hazell, A.; Jensen, K. B.; McKenzie, C. J.; Toftlund, H. *J. Chem. Soc., Dalton Trans.* **1993**, 3249−3257. (d) Dong, Y.; Fujii, H.; Hendrich, M. P.; Leising, R. A.; Pan, G.; Randall, C. R.; Wilkinson, E. C.; Zang, Y.; Que, L., Jr.; Fox, B. G.; Kauffmann, K.; Münck, E. *J. Am. Chem. Soc.* **1995**, *117*, 2778−2792.

(7) (a) Chen, S.; Richardson, J. F.; Buchanan, R. M. *Inorg. Chem.* **1994**, *33*, 2376−2382 and references therein. (b) Hendricks, H. M. J.; Birker, P. J. M. W. L.; Verschoor, G. C.; Reedijk, J. *J. Chem. Soc., Dalton Trans.* **1982**, 623−631. (c) Nishida, Y.; Watanabe, I.; Unoura, K. *Chem. Lett.* **1991**, 1517−1520.

(8) Oberhausen, K. J.; Richardson, J. F.; Buchanan, R. M.; Pierce, W. *Polyhedron* **1989**, *8*, 659−668.

(9) Sheldrick, G. M. *SHELXS86*; University of Göttingen, Göttingen, Germany, 1986.

(10) Sheldrick, G. M. *SHELXL*-93; University of Göttingen, Göttingen, Germany, 1993.

Table 1. Crystallographic Data for $[Fe(L)Cl_2]$

formula	$C_{12}H_{16}N_5FeCl_2O_2$
fw	389.05
crystal system	monoclinic
space group	$P2_1$
a (Å)	12.564(5)
b (Å)	25.960(10)
c (Å)	9.875(4)
α (deg)	90.00
β (deg)	90.494(4)
γ (deg)	90.00
V (Å^3)	3221(2)
Z	8
D_s (g/cm^{-3})	1.605
T (K)	293
crystal size (mm)	0.20 × 0.2 × 0.2
μ (mm^{-1})	1.281
F(000)	1592
theta range (deg)	2.06−19.98
scan type	$\omega/2\theta$
scan speed (deg·s^{-1})	0.08
index ranges	$-12 \le h \le 12$, $0 \le k \le 24$, $0 \le l \le 9$
reflections collected	2543
independent reflcns	2433 [R(int) = 0.1765]
refinement method	full−matrix least squares on F^2
data/restraints/parameters	2433/0/452
goodness-of-fit on F^2	0.904
$R1$	0.060 $I > 2\sigma(I)$
w$R2^a$	0.1479
maximum shift/esd	0.509
largest residual peak (e·Å^{-3})	0.644
lowest region (e·Å^{-3})	−0.527

[a] Weighting scheme: $w = [\sigma^2(F_o)^2 + (0.0776P)^2]^{-1}$ where $P = (F_o^2 + 2F_c^2)/3$.

Table 2. Selected Bond (Å) and Angles (deg) for $[Fe(L)Cl_2]$

		Bond Distances	
FeA−NA	2.32(2)	FeA−O(10A)	1.95(2)
FeA−N1A	2.09(2)	FeA−Cl(1A)	2.309(10)
FeA−N′1A	2.11(2)	FeA−Cl(2A)	2.262(8)
		Bond Angles	
NA−Fe−N1A	73.3(8)	N1A−Fe−Cl(2A)	108.6(6)
NA−Fe−N′1A	78.(8)	N′1A−Fe−O(10A)	84.2(8)
NA−Fe−O(10A)	874.6(7)	N′1A−Fe−Cl(1A)	172.1(6)
NA−Fe−Cl(1A)	94.9(6)	N′1A−Fe−Cl(2A)	90.1(6)
NA−Fe−Cl(2A)	168.2(6)	O(10A)−Fe−Cl(1A)	89.7(6)
N1A−Fe−N′1A	89.2(8)	O(10A)−Fe−Cl(2A)	108.6(6)
N1A−Fe−O(10A)	147.8(8)	Cl(1A)−Fe−Cl(2A)	96.5(4)
N1A−Fe−Cl(1A)	93.5(7)		

trile. Infrared spectra were recorded with a FTIR Bruker spectrophotometer as KBr disks. ^{1}H NMR and ^{13}C NMR spectra were obtained with a Bruker 200 spectrometer. Chemical shifts (in ppm) are referenced to the residual protic solvent peaks. X-band EPR spectra were obtained at liquid helium temperature with a Bruker ER-200D spectrometer equipped with an Oxford Instruments flow cryostat. The magnetic field was determined with a Hall probe, and the klystron frequency was determined with a Hewlett-Packard frequency meter. The microwave attenuation was 10 dB, and the modulation amplitude was 2 G.

Electrochemical Experiments. All the chemicals were of high-purity grade. DMSO (Aldrich, 99.8%, water <0.005%) and DMF (Burdick and Jackson, high-purity solvent) were used without further purification and kept in a glovebox under an argon atmosphere prior to use. Bu_4NPF_6 (Aldrich) was dried at 80 °C under vacuum for 3 days. For anaerobic conditions, the solutions were deaerated thoroughly for at least 30 min with pure argon and kept under a positive pressure of this gas during the experiments. Otherwise, the solutions were saturated with air (N 50 Air Liquide) or pure oxygen (N 48 Air liquide). The working electrode was a freshly polished glassy carbon disk (GC, Tokai, Japan, 3 mm diameter) for cyclic voltammetry or a large surface area glassy carbon plate (V25, Le Carbone Lorraine) for controlled potential electrolysis and coulometry. The reference electrode (SCE) was kept in a compartment containing the appropriate supporting electrolyte and was separated from the working electrode compartment by a fine porosity glass frit. The counter electrode, a platinum gauze with a large surface area, when used for controlled potential electrolysis and coulometry, was kept in the same way as the reference electrode, in a compartment separated from the working electrode compartment by a medium porosity glass frit. The electrochemical setup was an EG $ G 273A driven by a PC with the 270 software.

Scheme 1. Synthetic route to ligand LH

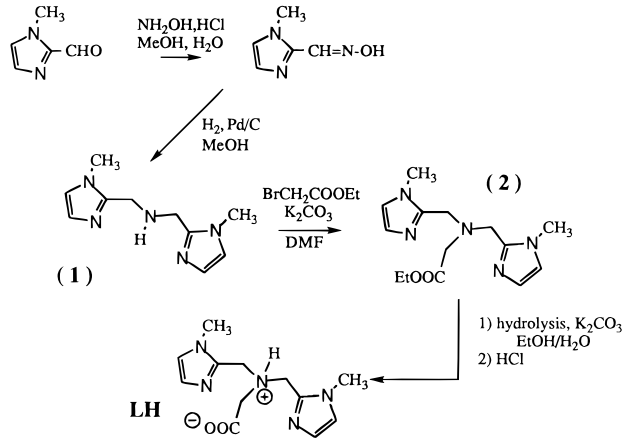

Results and Discussion

Syntheses. Attempts to synthesize the compound bis((1-methylimidazol-2-yl)methyl)amine (**1**) by the procedure described in the literature were unsuccessful[8] so we used a slightly modified method. Compound **1** was obtained directly from 1-methyl-2-imidazolcarboxaldehyde oxime by hydrogenation in nonanhydrous methanol by palladium/charcoal. Compound **2** was obtained by alkylation of **1**. The subsequent hydrolysis of **2** was performed to yield the ligand LH, as outlined in Scheme 1. The iron(III) complex was readily prepared by mixing equimolar amounts of iron(III) chloride and LH and half an equivalent of piperidine in MeOH under anaerobic conditions. Suitable crystals for X-ray analysis were obtained from an acetonitrile/methanol mixture, without addition of piperidine.

Crystal Structure. The crystal structure reveals mononuclear neutral molecules with four chiral molecules per asymmetric unit, related by pseudo but not crystallographic symmetry operators (center and helical axes). An ORTEP plot of both enantiomers is shown in Figure 1. The iron(III) center is located in a distorted octahedral environment consisting of four donor atoms from the ligand **L**, two imidazole nitrogen atoms, an amine nitrogen, and one oxygen of the carboxylate group, with the 6-fold coordination being completed by two chloride anions, as shown in Figure 1. The coordination of the carboxylate group was already verified by the IR spectrum. The difference, Δ, between the ν_{as}(C═O) and the ν_s(O−C−O) vibrations has been found to be larger than 200 cm^{-1}, suggesting that the carboxylate is bound in a monodentate way.[11] The following average bond lengths are evaluated from the bond lengths of the four entities in the asymmetric unit. The average Fe−N_{amine} bond length is 2.32 Å; it is slightly shorter than those found in $[Fe(H_2O)_2$-$TMIMA)_2O]^{4+}$ (2.38 Å).[6b,12] The average Fe−$N_{imidazole}$ bond length, equal to 2.08 Å, is smaller than that of the Fe−N_{amine} bond but comparable to the Fe−N_{im} found in $[Fe(H_2O)_2$-$(TMIMA)_2O]^{4+}$ (2.07 Å). We also noticed that the Fe−N_{im} bond is shorter than the Fe−N_{py} bonds, which are reported in all of the tripodal ligand-containing complexes having pyridine

(11) Beacon, G. B.; Phillips, R. J. *Coord. Chem. Rev.* **1980**, *33*, 227−250.
(12) TMIMA: *N*,*N*,*N*-tris(2-(1-methylimidazolyl)methyl)amine; BPG: *N*,*N*-bis(2-pyridylmethyl)glycine; DBC: 3,5-di-*tert*-butylcatecholate.

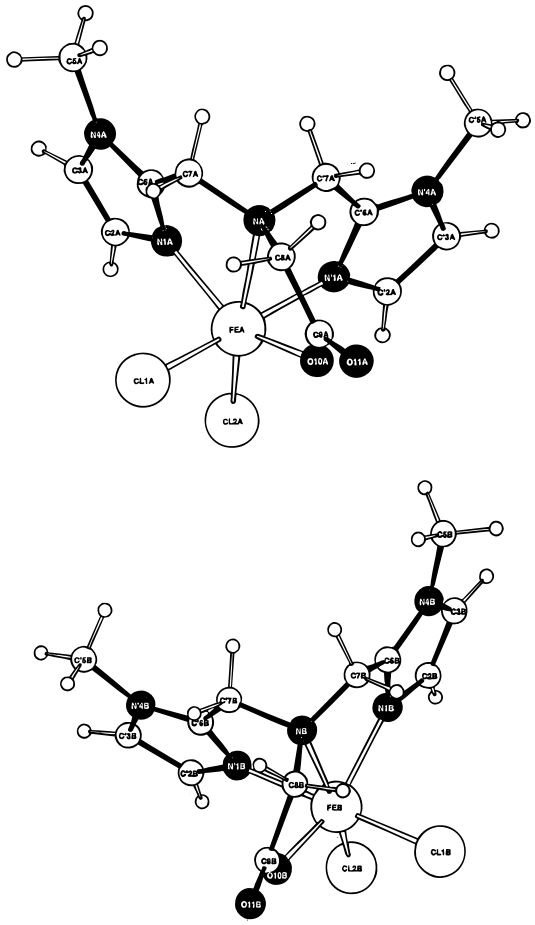

Figure 1. ORTEP view of the two $[Fe(L)Cl_2]$ enantiomers with labeling scheme. The hydrogen atoms are omitted for clarity.

instead of imidazole or carboxylate as the pendant arms. This suggests that imidazole is a better ligand than pyridine as proposed previously.[13] The average Fe−O bond length (1.96 Å) is similar to that found for [Fe(BPG)DBC].[5a] Due to the trans influence, the Fe−Cl1 bond length (2.332 Å) is significantly longer than that of Fe−Cl2 (2.255 Å). The distorsion in the coordination geometry is reflected in the bond angles. The average of the N_{amine}−Fe−N_{im} (76.5°) and N_{amine}−Fe−O (74.7°) bond angles is much smaller than the ideal 90° value due to the constraints that are imposed by the tripodal ligand arrangement that forms five-membered chelate rings. The structure confirms the iron chelation by the ligand L and, more specifically, by one of the oxygen atoms of the carboxylate pendant arm, when most of the previously reported iron(III) mononuclear complexes of tripodal ligands contain only nitrogen donors.

Spectroscopic and Electrochemical Characterization. The electronic spectra of FeL were recorded in DMF, DMSO, and acetonitrile. They have charge transfer bands with absorption maxima wavelengths and corresponding molar absorbances as given in Table 3. The spectra are strongly solvent dependent; two labile positions are occupied by the potentially exchangeable chloride anions. (See Figure 4 where the spectrum run in DMSO is shown.)

The EPR spectra of the complex FeL (Figure 2) are also solvent dependent. The spectrum run in a frozen aqueous solution (Figure 2A) is characterized by two predominant features at effective *g* values equal to 4.3 and 6.1 and by a broad

Table 3. Spectral Data for $[Fe(L)Cl_2]$: λ (nm) (ϵ, M^{-1} cm^{-1})

	DMSO	DMF	CH_3CN
$[Fe(L)Cl_2]$	303 (6900)[a]	308.5 (8410) 355 (4514) sh	248 (7190) 306 (5950) 332 (4620)

[a] Data in parentheses are extinction coefficients.

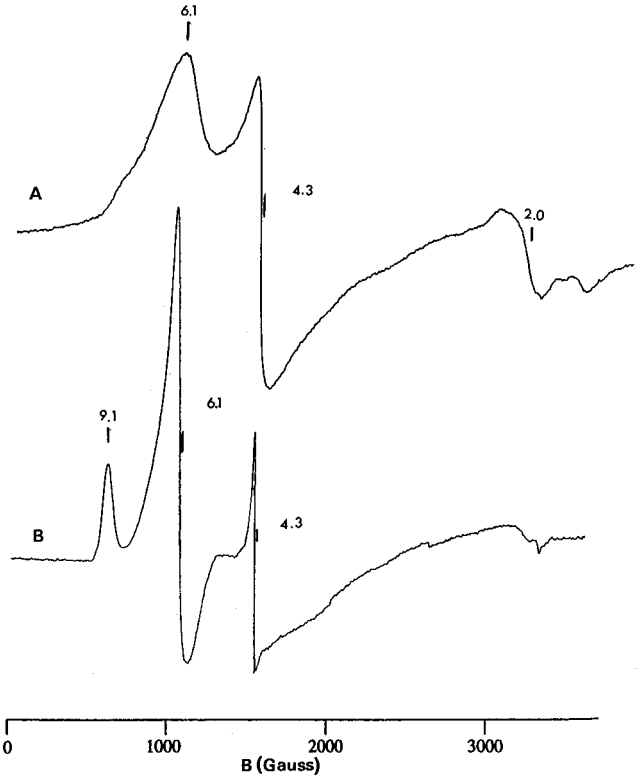

Figure 2. X-band EPR spectra of frozen solutions of $[Fe(L)Cl_2]$: (A) in water, (B) in water/propanediol (3:1). Instrumental conditions: microwave attenation, 10 dB; modulation amplitude, 2 G; temperature 4.2 K. Approximate effective *g* vales are indicated.

signal around $g = 2$. This indicates a mixture of high-spin molecules with either rhombic or axial symmetry. When the spectrum is run in a water/propanediol (3:1) solution, it is much better resolved. The signal near 6 becomes predominant (Figure 2B) while the relative amplitude of the signal at 4.3 decreases, and a new relatively intense signal is observed at 9.1. In addition to mononuclear molecules of rhombic symmetry, molecules of axial symmetry might also be present. Another explanation could be the formation of molecules of higher nuclearity. Similar spectra have been reported for polynuclear active sites with high-spin states arising from possible metal interactions.[14] Further work is in progress to gain an understanding of the nature of the species present in water solution.

Cyclic voltammograms were run in DMSO and in DMF containing 0.1 M NBu_4PF_6 as the supporting electrolyte. Figure 3 shows the main features observed in solutions that were thoroughly degassed with argon. The cyclic voltammogram in Figure 3a was obtained in DMSO. It exhibits a chemically reversible one-electron wave featuring the Fe(III)/Fe(II) redox process. The process is quasi-reversible, with $E° = -0.015$ V *vs* SCE, and the anodic to cathodic peak potential differences, ΔE_p, are slightly larger than 60 mV and increase with the scan rate. It is worth noting that the redox potential of the Fe(III)/Fe(II) system is close to 0 V *vs* SCE. This seems to be characteristic of the iron complexes with tripodal ligands.[15]

(13) Oberhausen, K. J.; O'Brien, R. J.; Richardson, J. F.; Buchanan, R. M. *Inorg. Chim. Acta* **1990**, *173*, 145−154.

(14) Pilbrow, J. R. In *Transition Ion Electron Paramagnetic Resonance*; Oxford Science Publications, Oxford, 1990.

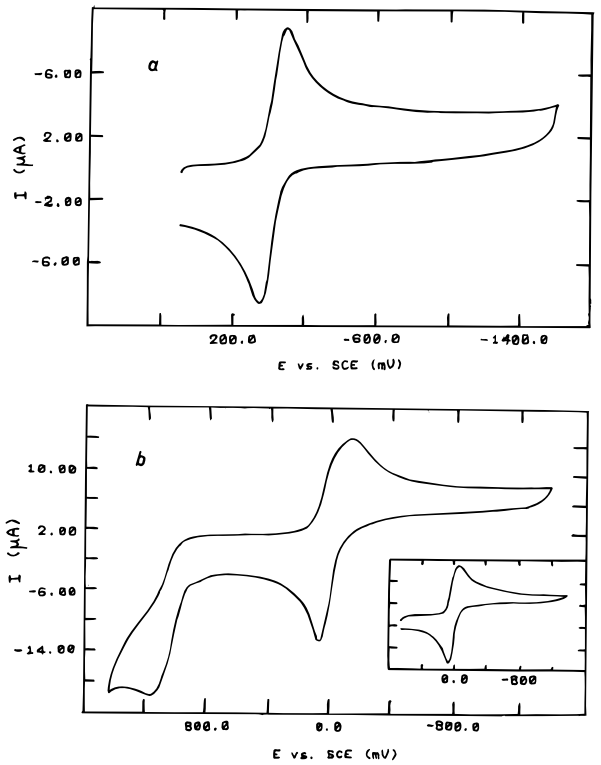

Figure 3. Cyclic voltammograms for 10^{-3} M [Fe(L)Cl_2]: (a) in DMSO and 0.1 M *n*-Bu_4NPF_6. (b) in DMF and 0.1 M *n*-Bu_4NPF_6. Working electrode was freshly polished glassy carbon electrode. Reference electrode was SCE. Scan rate: 200 mV/s. Solutions were thoroughly degassed with dry argon. Inset: scan rate $\upsilon = 20$ mV/s. The potential scan was restricted to the Fe(III)/Fe(II) domain.

Provisionally, we note that the average value of the redox potential of the Fe(III)/Fe(II) couple in native superoxide dismutases is found to be equal to +0.27 V *vs* NHE (+0.03 V *vs* SCE).[16] The cyclic voltammogram that was obtained in DMF is shown in Figure 3b. Several differences appear with DMSO. It was possible to extend the potential scan to more positive values in DMSO to observe a chemically irreversible oxidation wave with $E_{pa} = +1.15$ V *vs* SCE, corresponding to the imidazole moiety. The reduction wave of the Fe(III)/Fe(II) couple is a composite involving overlapping peaks. This observation may be traced to the possible existence of two Fe(III) species, one with DMF as a ligand and the second with Cl^- as a ligand.[17] In support of this assumption, we found, for instance, that addition of 2 M LiCl to the solution results in the observation of a single reduction wave at a more cathodic potential. Tentatively, the difference in the behavior of the complex in the two solvents might be ascribed to the difference in the donor numbers of DMSO and DMF, which is in favor of the former.[18] In DMF, an increase of the scan rate induces a larger separation of the two reduction peaks, the more cathodic one increasing faster than the other. By contrast, the inset in Figure 3b shows that an apparently single reduction wave is observed at a scan rate of 20 mV/s.

Reactivity toward Dioxygen and Superoxide. The interaction of the complex with dioxygen and superoxide has been considered and investigated through spectroscopic and electrochemical studies.

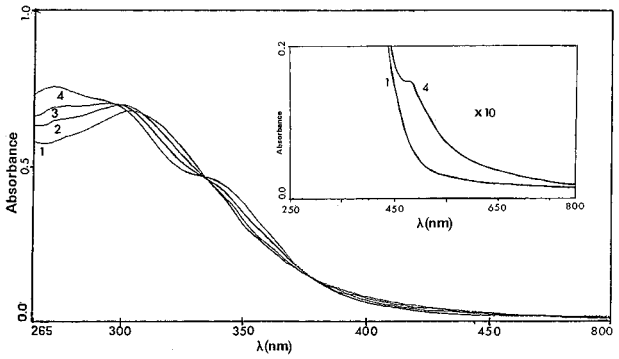

Figure 4. UV−vis spectra demonstrating reaction of [Fe(L)Cl_2] with KO_2 in DMSO: Curve 1, [Fe(L)Cl_2] complex without additon of KO_2; Curve 2, [KO_2]/[FeL] = 0.35; Curve 3, [KO_2]/[FeL] = 0.70; Curve 4, [KO_2]/[FeL] = 1. Inset: Comparison of spectra **1** and **4** at higher concentrations (×10).

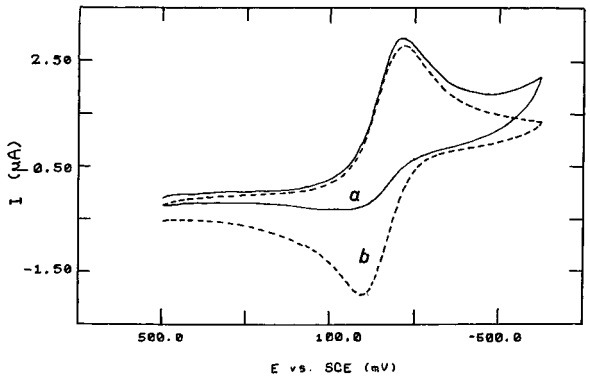

Figure 5. (a) Influence of dioxygen on first redox couple of [Fe(L)-Cl_2] in DMSO. (b) Cyclic voltammogram in presence of argon added for the sake of comparison. Working electrode: freshly polished glassy carbon electrode. Reference electrode: SCE. Scan rate: 20 mV/s.

Direct reaction of the complex with potassium superoxide in anhydrous and deoxygenated DMSO has been carried out, and the reaction was followed by UV−vis spectroscopic measurements (Figure 4). It is clearly shown that the complex reacts with superoxide to give a new product, the spectrum of which (spectrum 4) is characterized by three absorptions at 273, 295 and 334 nm. At higher concentrations, a small absorption appears at 471 nm, as shown in the inset of Figure 4. The maximum intensity is observed for the [KO_2]/[complex] ratio equal to 1, that corresponds to the new entity abbreviated [Fe^{III}−O_2^-]. As shown in Figure 4, an isosbestic point is observed at 333 nm, indicating that only two species are in equilibrium. The addition of larger amounts of superoxide to the solution resulted in a decay of the observed bands, probably due to the decomposition of this new complex and/or the formation of new species.

The reactivity of dioxygen with the reduced form of the complex has been investigated through electrochemical experiments.[19] Two cyclic voltammograms obtained in DMSO with either argon or oxygen bubbled through the solution prior to their recording are compared in Figure 5. In the presence of dioxygen, after the reduction of the Fe(III) species to the Fe(II) species, an oxidation trace does not occur on potential reversal. This observation unambiguously indicates that the Fe(II) species is removed from the electrode surface by a reaction with dioxygen. Furthermore, the current increase that is observed roughly 150 mV past the Fe(III)/Fe(II) peak suggests the presence of a new reducible species which did not build up

(15) Nishida, Y.; Watanabe, I.; Unoura, K. *Chem. Lett.* **1994**, 1721−1724.
(16) Barrette, W. C.; Sawyer, D. T.; Fee, J. A.; Asada, K. *Biochemistry* **1983**, *22*, 624−627.
(17) Szulbinski, W. S.; Warburton, P. R.; Busch, D. H. *Inorg. Chem.* **1993**, *32*, 297−302.
(18) Gutmann, V. *The Donor-Acceptor Approach to Molecular Interactions*; Plenum Press: New York, 1978.
(19) Sawyer, D. T. In *Oxygen Chemistry*; Oxford University Press: New York, 1991.

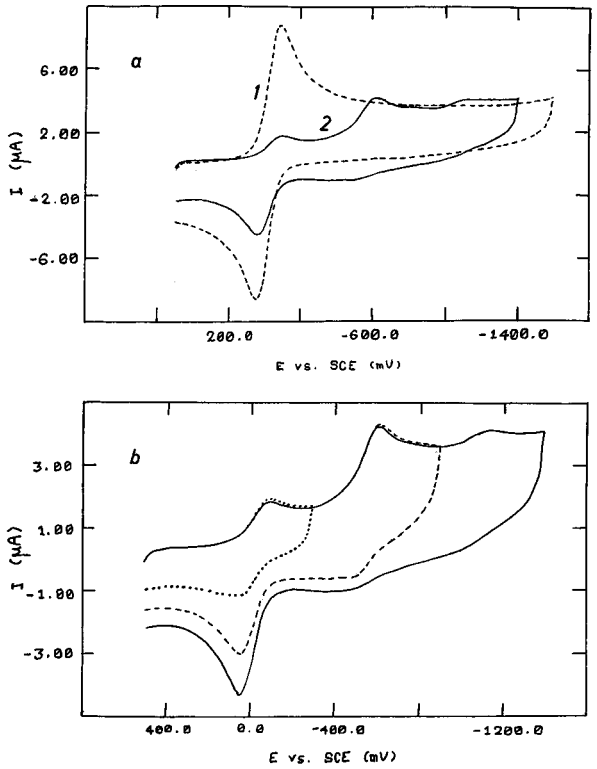

Figure 6. Cyclic voltammograms at a scan rate of 200 mV/s in DMSO under argon. Electrodes are the same as those in Figure 5. (a) Curve 1 is the initial $[Fe(L)Cl_2]$ complex; curve 2 was obtained after nearly exhaustive reduction of the Fe(III) to Fe(II) species, then bubbling with dioxygen, and finally degassing thoroughly with argon. (b) Detailed voltammetric study of curve 2 of Figure 6a showing that the main reduction product is oxidized at the same potential as the original Fe(II) species.

during reduction when the solution was degassed with argon. This current increase occurs in a potential domain in which no direct reduction of dioxygen on the electrode surface is possible. The following controlled potential coulometry experiments along with the associated cyclic voltammograms clearly confirm the buildup of this new species. Under strictly anaerobic conditions, controlled potential coulometry converts the Fe(III) species into the Fe(II) species after the uptake of 1 F/mol, as expected. Figure 6 illustrates two typical states of the species in solution. Curve 1 of Figure 6a shows the initial voltammogram recorded in anaerobic conditions prior to electrolysis. Curve 2 of Figure 6a has been recorded in the same solution after nearly exhaustive reduction of the Fe(III) species to Fe(II), then bubbling dioxygen thoroughly through the solution and finally degassing again with argon before the voltammetric scan. This direct comparison verifies the formation of a new species that is stable even in the absence of dioxygen and that is reducible at a more negative potential than that for the Fe(III) species. Figure 6b is interesting because it stresses that the reduction process of the new species under an argon atmosphere results in the formation of compounds that are oxidized mainly at the same potential as the original Fe(II) form of the complex. As a first step in the buildup of the species, a $Fe(II)-O_2$ complex is probably formed. The UV−vis spectrum in DMSO of this new species and the one shown in Figure 4 (spectrum 4) that was synthesized by adding an equimolecular amount of potassium superoxide to the starting Fe(III) complex are superimposable.

The reactivity of superoxide with the iron(III) complex was also monitored directly in the following experiment: a DMSO solution containing 0.1 M Bu_4NPF_6 was saturated with potassium superoxide.[20] Then the superoxide oxidation was monitored by cyclic voltammetry over a relatively long period of time and was found to give a reproducible peak current intensity. Aliquots of the Fe(III) complex were added successively and were found to induce a concomitant decrease of the superoxide oxidation wave. Another conformation of the reactivity of the superoxide anion was sought directly by the cyclic voltammetry experiments illustrated in Figure 7. The initial Fe(III) solution was thoroughly electrolyzed under argon to the Fe(II) state. Then the solution was saturated with air before running the cyclic voltammogram. Two remarks are important. First, the oxidation wave at +0.58 V does not appear until an excess of superoxide is generated at the electrode surface during the cathodic run. Second, part of the superoxide is oxidized during the potential scan in the positive direction, as also observed in the oxidation of the newly formed species. Therefore, the products in solution do not bring about any fouling and/or blocking of the electrode surface.

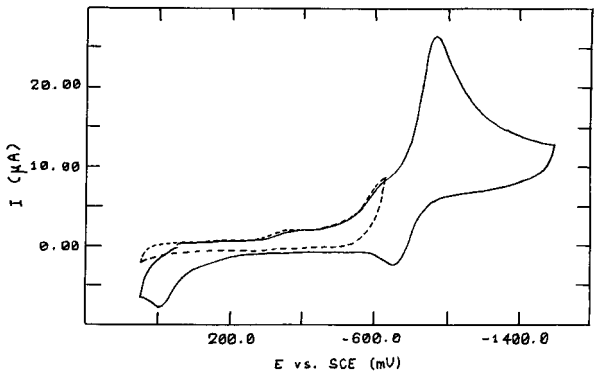

Figure 7. Cyclic voltammograms at a scan rate of 200 mV/s in DMSO solution, thoroughly degassed with dry argon. Electrodes are the same as those in Figure 5. The voltammograms were obtained after nearly exhaustive reduction of the Fe(III) to Fe(II) species and then bubbling with air. Comparison of these voltammograms shows the appearance of an oxidizable species when the cathodic potential run is extended up to the generation of superoxide.

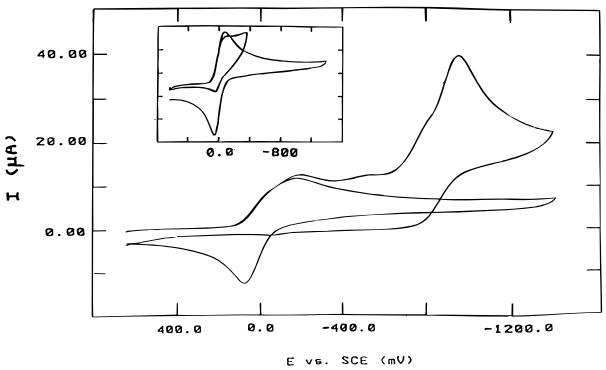

Figure 8. Cyclic voltammogram for 10^{-3} M $[Fe(L)Cl_2]$ in DMF and 0.1 M *n*-Bu_4NPF_6 and in the presence of $\approx 10^{-3}$ M O_2. The wave obtained in the absence of O_2 is added for the sake of comparison. Scan rate: 200 mV/s. The electrodes are the same as in previous figures. Inset: scan rate = 20 mV/s. The waves are restricted to the Fe(III)/Fe(II) couple in the absence of oxygen and in the presence of $\approx 10^{-2}$ M O_2, respectively.

All of the aforementioned results are perfectly in line with the observations made in DMF. Completely parallel observations are made in the two solvents. Figure 8 shows that dioxygen as well as superoxide prove to be reactive toward the complex.

(20) Szulbinski, W. S.; Warburton, P. R.; Busch, D. H. *Inorg. Chem.* **1993**, *32*, 5368−5376.

The reactivity studies we have performed demonstrate that the reaction of $Fe^{III}L$ with superoxide produces the same species as the reaction of $Fe^{II}L$ with dioxygen. In porphyrin chemistry, the formation of iron(III)$-O_2^-$ adducts equivalent to iron(II)$-O_2$ adducts has been observed already.[21] In non-heme chemistry, few iron(II) complexes have been reported to react with oxygen and form stable adducts that ultimately may produce dinuclear iron(III)−peroxy species.[22] The nature of the newly discovered species is under current investigation.

Conclusion

In summary, the reported complex is the first model of a mononuclear non-heme iron complex containing active sites, with the iron(III) ion being chelated by a tripodal tetradentate ligand which associates carboxylate and imidazole functions as the pendant groups. Spectroscopic and electrochemical studies have been performed in order to investigate the reactivity of the molecule with dioxygen and superoxide. A stable oxygenated form of the complex, tentatively symbolyzed [$Fe^{III}-O_2^-$] or [$Fe^{II}-O_2$], has been discovered. Work in progress is aimed at the elucidation of the stoichiometry, the structure, and the reactivity of this new species.

Supporting Information Available: Tables of the crystal data and structure refinement, atomic coordinates, anisotropic thermal parameters, bond distances and angles, and hydrogen coordinates (13 pages). Ordering information is given on any current masthead page.

IC951060M

(21) McCandlish, E.; Miksztal, A. R.; Nappa, M.; Sprenger, A. Q.; Valentine, J. S. *J. Am. Chem. Soc.* **1980**, *102*, 4268.

(22) (a) Kitajima, N.; Tamura, N.; Amagai, H.; Fukui, H.; Moro-oka, Y.; Mitzutani, Y.; Kitagawa, T.; Mathur, R.; Heerwegh, K.; Reed, C. A.; Randall, C. R.; Que, L., Jr.; Tatsumi, K. *J. Am. Chem. Soc.* **1994**, *116*, 9071−9085. (b) Kitajima, N.; Fukui, H.; Moro-oka, Y. *J. Am. Chem. Soc.* **1990**, *112*, 6402−6403. (c) Sawyer, D. T.; McDowell, M. S.; Spencer, L.; Tsang, P. K. S. *Inorg. Chem.* **1989**, *28*, 1166−1170.